Research highlight

Khouloud Eledlebi*, Mohammed Ismail and Moh'd Rezeq

Finite element simulation and analysis of nanometal-semiconductor contacts

DOI 10.1515/ntrev-2015-0039
Received July 23, 2015; accepted October 7, 2015; previously published online May 16, 2016

Abstract: Nanometal-semiconductor contacts in the sub-20-nm range have shown some deviations in electrical characteristics compared to conventional diodes. We have used a finite element simulation software to build and analyze a proposed geometrical model. We used two different theoretical approaches to study the enhancements of the electric field at the interface, and then the total current across nano-Schottky junction. The results revealed a significant tunneling current at the reverse bias for low n-doped semiconductor substrates and low current at the forward bias. However, in the case of high n-doped semiconductor substrates, the thermionic current is significant at forward biases and the current is low at the reverse bias. We have used our finite element simulation models based on both approaches to fit the existing experimental data of nano-Schottky contacts.

Keywords: nanodevices; nanometal particles; nano-Schottky junctions; thermionic current; tunneling current.

1 Introduction

As the demand on compact electronic devices increases, growing numbers of research projects are being directed toward scaling down the size of basic device components, targeting the range of sub-20 nm. The size reduction of electronic devices is needed to increase the number of components on the same wafer, and to provide faster transmission of data at low power [1]. In fact, the smaller the device, the less energy is consumed, as the required operation voltage and current become much less [2]. Reducing the circuit capacitance, as the basic components (transistors) become smaller with shorter interconnections, leads to a decrease in the circuit delays. Moreover, the electronic devices become cheaper as the number of transistors on a single semiconductor wafer increases [3]. Therefore, researchers are interested in scaling down electronic devices, especially complementary metal oxide semiconductor devices, as they are the dominant components of existing technologies [4].

However, scaling down the size of basic device components is affected by several obstacles such as overlapping of the depletion regions of consecutive semiconductor junctions, the increase of gate leakage current, and the inability to control dopant concentrations on extremely small areas [5]. Devices based on nano-Schottky junctions could be an option to help in solving the previous issues [6, 7]. However, the conventional theory used for planar metal semiconductor contacts, which assumes planar physical boundary conditions at the interface, might not be applicable when the size of the contact is reduced to the sub-10-nm scale [8–10]. A new approach has been considered to account for metal-semiconductor (M-S) contacts at this range. The new analysis is based on the alignment of Fermi levels between metal and semiconductor bulks [11, 12].

The theoretical model for nano-M-S interfaces is built based on having nanometal particles embedded on the surface of semiconductor substrates. The theoretical model of the nano-Schottky junction is established to extract the important interface parameters, such as the electric field and the built-in potential, based on the conventional and new approaches [13–15]. Due to the enhanced electric field at the nano-M-S interface, the barrier width is narrowed and found to be within the range of the nanometal particle size. This, in turn, results in an enhancement in the tunneling current through the junction [13–15]. We have utilized a finite element simulation tool (COMSOL) to perform simulation analysis based on the previous model. The built model is used to calculate the total current at the interface and fit the experimental data to demonstrate the validity of this model [13–15]. The theoretical results showed good agreement with the experimental data of nano-Schottky junctions.

***Corresponding author: Khouloud Eledlebi,** Department of Electrical and Computer Engineering and KSRC Research Center, Khalifa University of Science, Technology and Research, Abu Dhabi, UAE, e-mail: khouloud.edlebi@kustar.ac.ae
Mohammed Ismail: Department of Electrical and Computer Engineering and KSRC Research Center, Khalifa University of Science, Technology and Research, Abu Dhabi, UAE
Moh'd Rezeq: Department of Applied Mathematics and Sciences, Electrical and Computer Engineering and KSRC Research Center, Khalifa University of Science, Technology and Research, Abu Dhabi, UAE

Before discussing the analysis of the new nano-M-S contact model, we briefly review the theory of the planar M-S contacts as follows: when a metal and n-doped semiconductor materials, for example, are brought into physical contact, the free electrons at the conduction band of the n-type semiconductor transfers to the metal, leaving behind a depletion region of positive charges in the semiconductor side, adjacent to the junction [6, 7]. This region continues to extend in the semiconductor bulk until an equilibrium state of Fermi levels is reached on both sides. This results in accumulation of a negative charge of the same amount on the surface of metal contact to maintain the charge conservation. The surface charge density on the metal side determines the maximum electric field at the interface. However, solving Poisson's equation is important to find the electric potential distribution, and hence the electric field profile, over the depletion region knowing the charge density and boundary conditions [16, 17]. Figure 1 schematically represents the energy band diagram of a planar M-S contact, where V_{bi} is the built-in potential at the interface and Φ_B is the barrier height of the Schottky contact.

Solving Poisson's equation over the depletion region to find the electrostatic variables, like the depletion width, the built-in potential, and the induced electric field at the interface, are crucial for describing the behavior of planar M-S contacts and the current transfer through the junction [16, 17]. In this work, we focus on special cases of M-S contacts, especially when the metal contact is in the sub-20-nm range, as we stated earlier.

2 Simulation model

To analyze M-S contacts at the nanoscale, the most feasible model is visualizing the metal contact as a nanosphere embedded in a semiconductor bulk. A similar approach was adopted by Smit et al. [8–10], in which the spherical symmetry of the model is utilized to solve Poisson's equations. Figure 2 schematically shows a two-dimensional (2D) representation of the physical contact between a hemispherical metal surface and a semiconductor surface, where W_n is the depletion width of the nano-M-S contact model, $V(R)$ is the potential at the surface of the metal particle, and $V(R+W_n)$ is the potential at the end of the depletion width.

Two approaches are introduced for the analysis. The first approach (approach 1) is based on the conventional analysis, where the potential at the interface is fixed at the barrier height, and inside the bulk (at the end of the depletion region) the potential is ϕ_s (where $\phi_s = \frac{(E_C - E_F)}{q}$). These boundary conditions are used in Poisson's equation to solve for the depletion region and for finding the electric field at the interface. The calculations of W_n are done for several metal radii, to ensure that the model converges to the planar M-S contact. Figure 3 shows calculations for a low n-doped semiconductor substrate, where W_n increases smoothly from a small value (3 nm) until it reaches the conventional range (50 μm) at large radius [12].

The second approach is based on the alignment between the Fermi levels of the metal with the semiconductor and on the evolution of the potential profile, as the size of the interface decreases from the planar range into the nanoscale range [11, 13]. This model is referred to as the modified approach (approach 2), where the potential is not fixed at the interface, particularly when the metal contact has a limited nanoradius or <30 nm (this value depends on the bulk dopant concentration). Although the

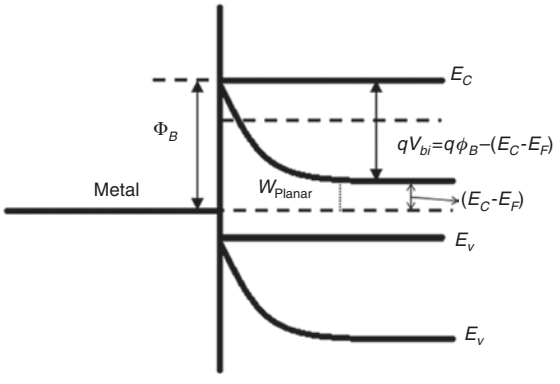

Figure 1: A schematic of a planar M-S contact at the equilibrium state.

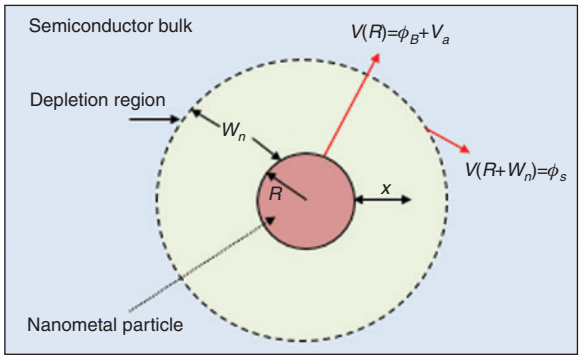

Figure 2: A schematic showing the top view (2D model) of a hemispherical nanoparticle embedded in the surface of a semiconductor substrate [11].

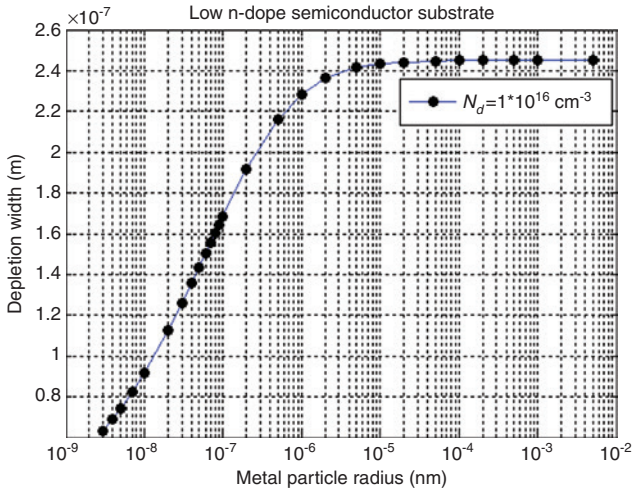

Figure 3: The depletion width values for model 1 as the metal radius increases from 3 nm to 50 μm for low n-doped substrate. The horizontal scale is logarithmic.

amount of charge transferred from the semiconductor to the nanometal particle is much less than that in planar M-S contacts, the surface charge density will be higher [11]. The electric potential also drops faster, as the radius of the spherical contact decreases, which means higher electric field at the interface. The evolution of the potential energy diagram is illustrated schematically in Figure 4, where ϕ_{on} denotes the new surface potential energy. The potential drop inside the bulk denoted by ΔV in Figure 4 is assumed to be proportional to the decrease of the contact size radius. Therefore, in our assumption, we relied on the evolution of the potential profile, as the fast drop of the potential is proportional to the nanometal radius sphere, and the high surface charge density. This increase in the surface charge density results in an enhancement of the potential at the interface and hence an enhancement in the electric field as shown in Figure 5 [13].

As the model contains nanospherical metal contact, Poisson's equation in the spherical coordinate system is used to solve for the depletion width (W_n):

$$\nabla^2 V = \frac{1}{r^2}\frac{\partial}{\partial r}\left(r^2\frac{\partial V}{\partial r}\right) + \frac{1}{r^2 \sin\theta}\frac{\partial}{\partial \theta}\left(\sin\theta\frac{\partial V}{\partial \theta}\right) + \frac{1}{r^2 \sin^2\theta}\frac{\partial^2 V}{\partial \varnothing^2} = -\frac{\rho_v}{\varepsilon_S}, \quad (1)$$

where ρ_v is the space charge density of the semiconductor bulk and ε_S is the semiconductor permittivity. The model is assumed to be symmetric in the spherical coordinate system. Hence, the potential and the electric field do not change with the change of θ or $\varnothing$. Consequently, the equation can be reduced to be dependent on one variable (r):

$$\nabla^2 V = \frac{1}{r^2}\frac{\partial}{\partial r}\left(r^2\frac{\partial V}{\partial r}\right) = -\frac{\rho_v}{\varepsilon_S}, \quad (2)$$

where r is the variable referred to as ($R+W_n$), as in Figure 11, that is solved for to get the depletion width of the junction.

For the model analysis, a Matlab program is generated to calculate the depletion width for different metal particle radii spanning a range from nanoscale (3 nm) to conventional scale (50 μm). The calculations are done for low n-doped (in the order of 1×10^{18} cm^{-3}) and high (in the order of 1×10^{15} cm^{-3}) n-doped semiconductor substrates. The results showed that the modified approach produces

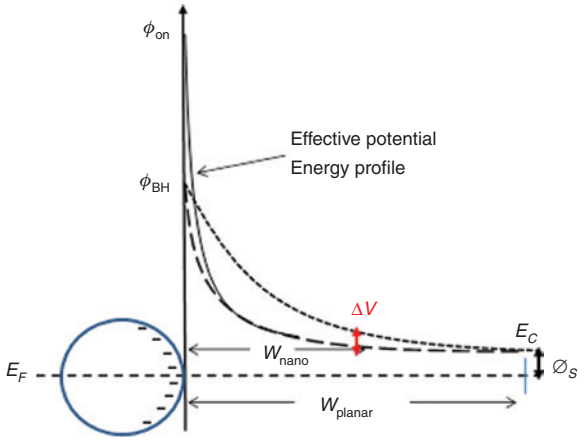

Figure 4: The effect of having high surface charge density on nanometal particle to the reduction in the depletion width over the planar value, which results in an improvement of the potential energy at the interface to a maximum value as ϕ_{on} [11].

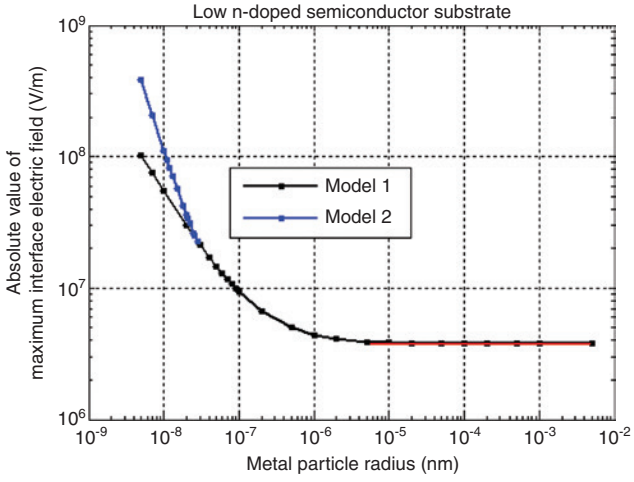

Figure 5: A schematic showing the maximum electric field at the M-S interface for a low n-doped substrate when the metal particle radius increases.

better data fit than the conventional one for nanometal contacts <30 nm on low n-doped Si substrates. This is because the potential at the interface is assumed to be proportional to the charge density on the nanometal surface, unlike the conventional approach, which assumes the potential to be pinned at the barrier height value. For metal nanoparticles of radii >30 nm, the depletion width for the modified approach converges to the values obtained by the conventional approach.

Figure 5 shows the calculated electric field at the nano-M-S interface, where the modified approach of nano-Schottky contact (approach 2) results in higher electric field at the interface compared to the conventional approach (approach 1). This is due to the relatively higher depletion width found from approach 2 compared to approach 1, and hence higher surface charge density on the metal surface. This higher electric field results in generating higher tunneling current at a reverse bias, as it will be demonstrated in the next section. Now for the case of high n-doped substrate, it is found as in Figure 6 that the depletion width of the nano-M-S contact for both models is the same, as the interface potential is found to be the same even for metal nanoparticle radius as small as 5 nm. This, in turn, leads to the same calculated I-V data, as we demonstrate in the next section.

3 Simulation analysis

The simulation models are generated using a COMSOL multiphysics program. The process included defining the geometry, meshing, specifying physical parameters, running the solutions, and then visualizing the results. Figure 7 shows a 3D model of the nano-Schottky contact geometry. COMSOL includes several predefined physics modules used for different applications. For example, the type of physics package used to implement the M-S contacts is Electrostatic Physics, which has Gauss's laws of flux and electric displacement fields. Charge distribution equations are available for defining the surface and space charges, and for conservation of charges. After building the geometrical model, materials for the two domains (metal and semiconductor) are defined. The metal domain material is set to gold, while the semiconductor material is silicon. After that, the parameters and variables used for finding the depletion width, electric field, and electric potential at the interface of the model are inserted in the program. Two different dopant concentrations were considered for n-doped semiconductor substrates (N_D=1×10^{16} cm^{-3} and N_D=1×10^{18} cm^{-3} for low n-doped and high n-doped substrates, respectively). The next step is defining the physics and mechanisms that COMSOL should solve for plotting the results. The program is set to solve for the electric field at the interface, after considering the main parameters like space charge density and surface charge density, the potential at the end of the depletion region.

The model is simulated to find the electric field at the interface. Figure 8 shows a 2D model of the nano-M-S junction with the variation of the electric field along the interface. The red color in Figure 8 indicates the maximum value of the electric field, and it decreases exponentially inside the semiconductor bulk. The main focus in the analysis is to get the maximum electric field value at the interface, which determines the tunneling current across the junction. Therefore, the program is set to select the

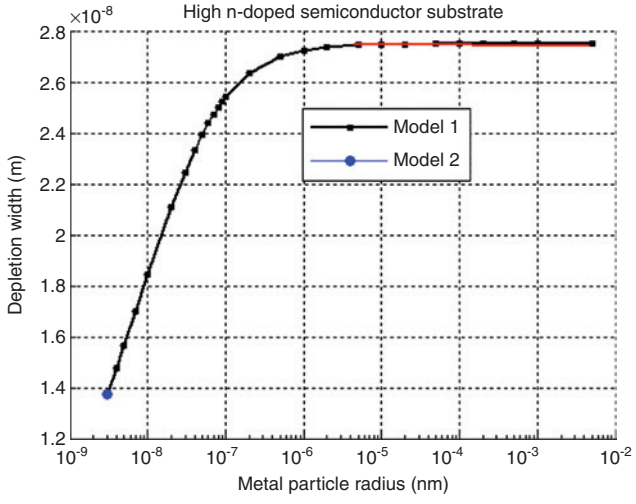

Figure 6: A schematic showing the changes in the depletion width of nano-Schottky junction for a high n-doped substrate as the metal particle radius increases.

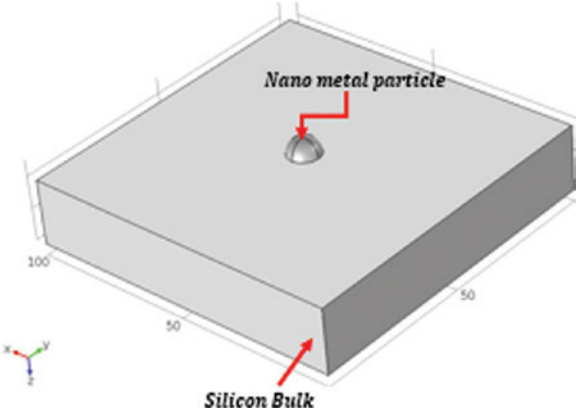

Figure 7: A schematic showing a 3D model for nano-M-S contacts created in COMSOL [15].

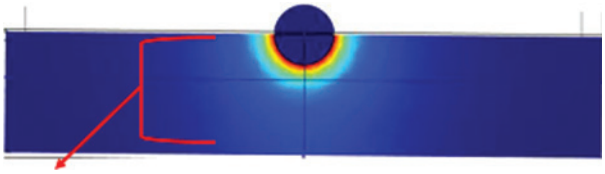

Figure 8: A 2D model showing the electric field inside the silicon bulk along the x-z plane [15].

maximum electric field to be used in the calculations of the total current. Then, the simulation model is set to vary the applied voltage along with its corresponding depletion width (w), as inferred from the theoretical model. The applied voltage is varied from -V to +V values, according to the range of the applied voltage used in the experiments, and the corresponding electric field is calculated using the established current theories, as explained in the next section.

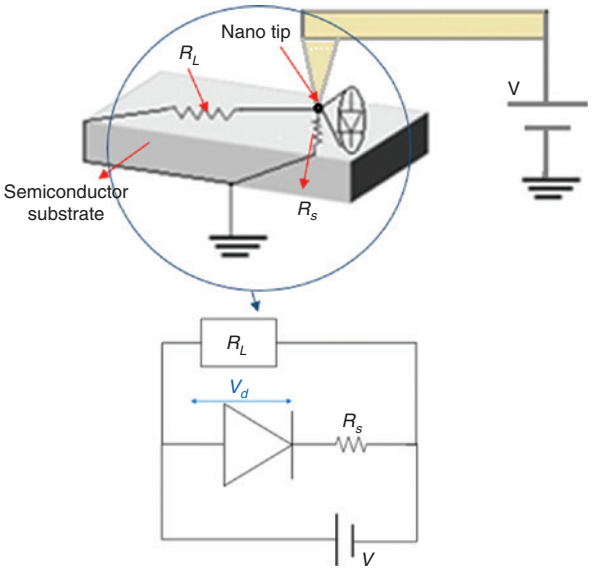

Figure 9: A schematic showing a nano-tip in contact with a semiconductor substrate and the contribution of series resistance and surface resistance with an equivalent circuit representation.

4 Experimental measurements and data fitting

Nano-M-S contacts are experimentally investigated by using atomic force microscope (AFM) tips in the conductive mode. In the experiment, to ensure a conductive AFM tip, the tip is coated with 5–20 nm layers of gold using physical vapor deposition method under modest vacuum conditions [13]. The tip is then characterized in the helium ion microscope, which is known for its higher resolution and better image contrast compared to electron microscopes [13]. Tips with a well-defined shape structure and a radius around 10 nm have been selected for the measurements. The experimental setup is illustrated schematically in Figure 9. When the tip is making contact with the substrate surface, there is spreading contact resistance referred to as a spreading resistance (R_S) [19–25]. There is also a chance of having a surface leakage current due to the surface conductance with a resistance referred to as R_L, which is inversely proportional to surface conductance (G_P) [18]. These parameters are included in the simulation analysis to provide a better I-V data fit.

The I-V measurements are performed using the previous setup for two types of n-doped Si samples: low n-doped Si (5–10 Ω·cm) and high n-doped Si (0.02–0.04 Ω·cm), where the direct current voltage is applied on the silicon substrate [13–15]. The measurements are done in two different sample preparation environments and classified into two categories: low contact resistance (where there is a relatively good physical contact between the nanotip and the surface of the substrate) and high contact resistance (due to a poor physical contact between the nanotip and surface, which is probably due to some contaminations on the surface of the substrate).

4.1 Low contact resistance

The I-V measurements are performed on low n-doped and high n-doped Si substrates. The voltage is swept between -0.8 V and 0.8 V. The experimental data for low n-doped substrate is represented in Figure 10 (denoted by red line), which shows a reversed rectification behavior compared to conventional nano-Schottky contact with n-doped Si substrates.

The same measurements are performed on high n-doped Si substrate, and the data are presented in Figure 11. One can easily notice that the experimental I-V behavior (red solid curve) is similar to the conventional I-V characteristics, where the current in the reverse bias is almost negligible and the current in the forward bias is significant.

4.2 High contact resistance

For this category of I-V measurements, the current value is much less than that obtained for low-resistance contacts. The I-V measurements are conducted for low n-doped and

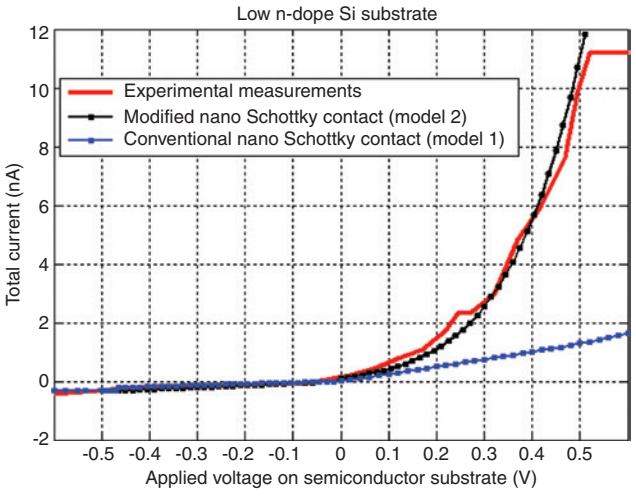

Figure 10: I-V data of the nano-Schottky junction between a nanotip and a low n-doped semiconductor substrate.

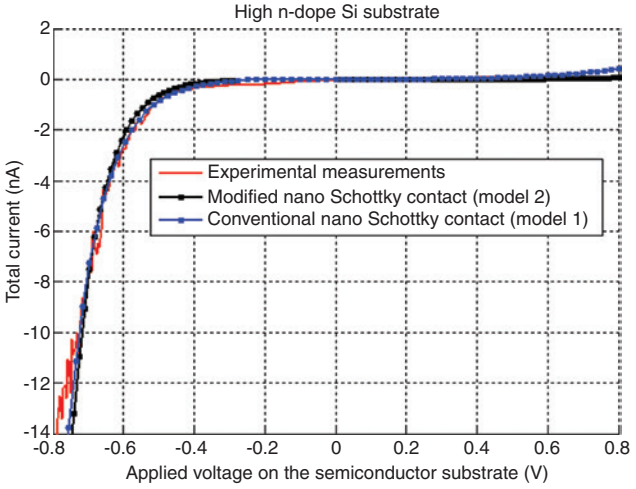

Figure 11: I-V data of the nano-Schottky junction between a nanotip and a high n-doped semiconductor substrate.

high n-doped Si substrates. This time, the voltage is swept between -1.0 V and 1.0 V. The experimental data for low n-doped Si substrate is presented in Figure 12 (denoted by red solid curve). The data clearly show that the tunneling current in the reverse bias is enhanced, leading to a reversed rectification behavior compared to conventional nano-Schottky contacts, which is consistent with the previous observations.

The same measurements are performed on high n-doped Si substrates, and the data are presented in Figure 13. It can be easily noticed that the experimental I-V behavior (red solid curve) is similar to the conventional Schottky diode I-V characteristics, where the current in the reverse bias is almost negligible and the current in the forward bias is significant.

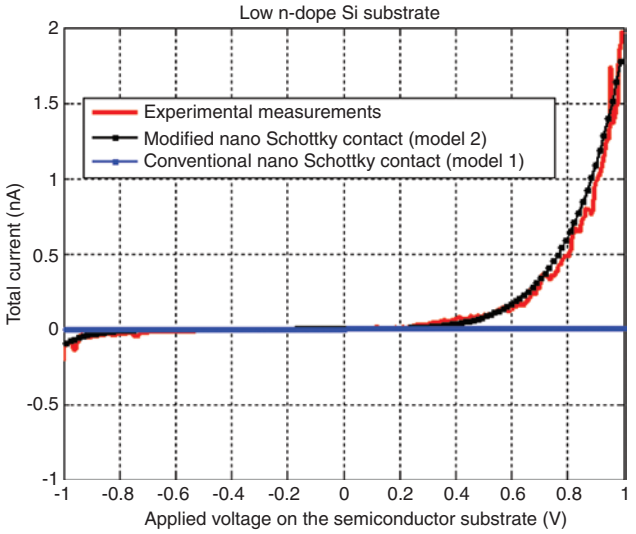

Figure 12: I-V data of the nano-Schottky junction between a nanotip and a low n-doped semiconductor substrate. The data show high contact resistance.

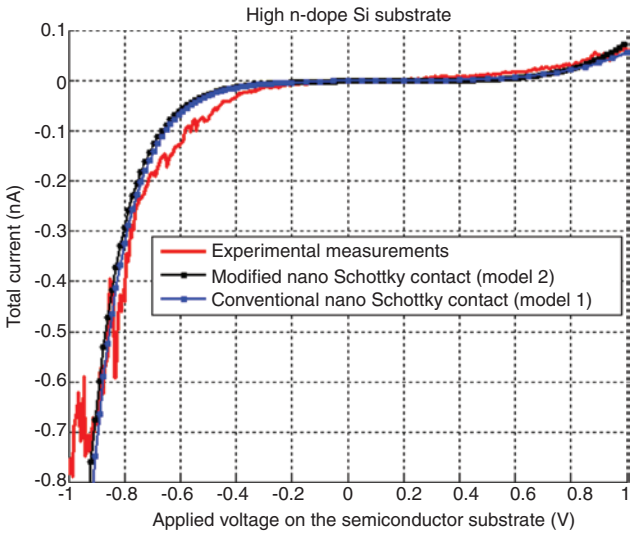

Figure 13: I-V data of the nano-Schottky junction between a nanotip and a high n-doped semiconductor substrate. The data show high contact resistance.

4.3 Data fitting and simulation results

By fitting the data using the simulation model, we can extract the main parameters such as the contact area (A), series resistance (R_s), surface resistance (R_L), and ideality factor (n) as follows. The data fitting starts by looking at the experimental I-V in the forward bias, as the thermionic current is expected to be dominant, especially at a forward bias >0.1 V. The estimation of the contact area is made from the tip radius and the thermionic current in the

forward bias. The ideality factor affects the turning point, and it is assumed to be of value 1, which is consistent with the value used previously in the literature [18, 19]. The surface leakage current has an ohmic behavior, and it can be observed from the linear part at a small voltage range around the origin. The surface resistance is estimated to be around 500 MΩ for low contact resistance measurements and in the order of 1 GΩ for high contact resistance measurements.

Referring to our model in Figure 9, the diode and contact resistance are arranged in series; hence, the applied voltage is divided between them. This means that the experimental current value at a given applied voltage in the forward bias is actually due to an effective voltage on the diode (V_d), which is less than the applied voltage. In other words, the total applied voltage (V_{app}) equals the effective applied voltage on the diode plus the voltage applied on the series resistance. To find the effective applied voltage, we first used the summation of the tunneling current and thermionic current as follows:

Thermionic current equation [6, 7]:

$$I_{th}=A.A^{*}T^{2}e^{\left[\frac{-q\phi_b}{kT}\right]}\left[e^{\frac{q(V-I_{th}R_S)}{nkT}}-1\right]+\frac{V}{R_L}. \quad (3)$$

Tunneling current equation [6, 7]:

$$I_{tun}=A.\frac{q^2E_{max}^{\ 2}}{8\pi\hbar(\Phi_B)}e^{\left[\frac{8\pi}{3hqE_{max}}\sqrt{2m^{*}(q(\Phi_B))^3}\right]}, \quad (4)$$

where A is the cross-section area of the metal particle inside the semiconductor bulk, A^{*} is Richardson's constant $\left(A^{*}=112\frac{A}{cm^2\times K^2}\right)$, Φ_B is the potential barrier height, V is the bias voltage, k is Boltzmann's constant (k=1.3806488×10^{-23} m^2 kg.s^{-2} K^{-1}), m^{*} is the effective mass of the semiconductor, n is the concentration of electrons, E_{max} is the maximum electric field at the interface, $\hbar$ is Planck constant ($\hbar$=6.62606957(29)×10^{-34} J.s), and T is the absolute temperature (T=300 K).

The value of R_S is estimated by considering the effective applied voltage on the diode (V_d), which gives the same experimental value of the total current. The series resistance is found to be around 20 MΩ for low contact resistance measurements and around 650 MΩ for high contact resistance measurements. These parameters (mainly, R_S, A, R_L, n) are then used to find the total current in the reverse bias, which is dominant by tunneling current. The estimated values of R_S are used to calculate the effective voltage on the diode in the reverse bias, by considering the difference between the experimental applied voltage (V_{app}) and the voltage drop on the series resistance (V_R), as follows:

$$V_d=V_{app}-I_{tot}R_S. \quad (5)$$

The same procedure is repeated for high n-doped substrate and for both set of measurements. Figures 10–13 show the best data fit for the experimental measurements. The high tunneling current observed on low n-doped substrate indicates an enhancement of the electric field at the nano-interface, hence a very thin tunneling barrier. Both approaches (the conventional approach and the modified approach) show a strong dependence of the electric field on the reduction of the size of the metal contact. However, the modified approach (approach 2) shows a better data fit in the reverse bias, particularly for low n-doped substrates. However, for high n-doped substrates, we have not seen any difference between both approaches. Both approaches show no effect when fitting the data in forward biases, as the current is dominant by thermionic current, which does not depend on the radius of the metal contact.

5 Conclusion

The I-V characteristics of nano-Schottky junctions are simulated using COMSOL multiphysics software. Two approaches are implemented on the theoretical model. The first approach is based on the conventional boundary conditions when solving Poisson's equation (assuming the potential at the interface is locked at the barrier height value, referred to as approach 1). The second approach is the modified approach of nano-Schottky junctions analysis, referred to as approach 2, which is based on the alignment of Fermi levels between the semiconductor and the metal at the nano-interface, and the evolution of the potential profile, as the contact size is reduced to nanoscale. Approach 2 shows better match with the experimental results compared to the conventional approach (approach 1), especially for low n-doped substrate, particularly at the sub-20-nm M-S contact scale. For low n-doped semiconductor substrate, a reversed rectification behavior is observed due to the enhancement of the electric field at the interface, and thus an enhancement in the tunneling current. Whereas the thermionic current in both models is calculated the same way for low n-doped and high n-doped semiconductor substrates, as it is independent on the contact size of the nanoparticle, which is dominant in the forward bias. This concept of nano-Schottky junctions can be used to build new types of basic electronic

devices and logic gates [19, 20]. These devices would be considered as low-power devices because the operation voltage and current are very small in the reverse bias.

Acknowledgments: The authors would like to thank Advance Technology Investment Company (ATIC), Abu Dhabi, and Semiconductor Research Corporation (SRC) for the financial support under ATIC-SRC grant number 2011-VJ-2333.

References

[1] Esmaeilzadeh H, Blem E, Amant RS, Sankaralingam K, Burger D. *Dark Silicon and the End of Multicore Scaling*. IEEE Computer Society: Washington, DC, 2012.
[2] Aizcorbe A, Kortum S. *Moore's Law and the Semiconductor Industry: A Vintage Model*. Harvard University: Cambridge, 2004.
[3] Auth C. 22-nm Fully-depleted tri-gate CMOS transistors. In *Custom Integrated Circuits Conference*. San Jose, CA, 2012.
[4] Hiroshi I. *Future of Nano-CMOS Technology*. Tokyo Institute of Technology: Tokyo, 2007.
[5] Narendra SG, Chandrakasan A. *Leakage in Nanometer CMOS Technologies*, vol. 307. Springer: New York, 2006.
[6] Sze SM. Metal-semiconductor contacts. In *Physics of Semiconductor Devices*. Wiley-Interscience Publication: NJ, 1981, pp. 245–260.
[7] Rhoderick EH, Williams RH. *Metal-Semiconductor Contacts*. Clarendon Press, Oxford University: NY, 1988.
[8] Smit GDJ, Rogge S, Klapwijk TM. Scaling of nano-Schottky-diodes. *Appl. Phys. Lett.* 2002, 81, 3852–3854.
[9] Smit GJ, Flokstra MG, Rogge S, Klapwijk TM. Scaling of micro-fabricated nanometer-sized Schottky diodes. *Microelectron. Eng.* 2002, 64, 429–433.
[10] Smit GDJ, Rogge S, Klapwijk TM. Enhanced tunneling across nanometer-scale metal-semiconductor interfaces. *Appl. Phys. Lett.* 2002, 80, 2568–2570.
[11] Rezeq M, Ismail M. The significant effect of the size of a nano-metal particle on the interface with a semiconductor substrate. In *12th IEEE International Conference on Nanotechnology (IEEE-NANO)*, Birmingham, UK, 2012.
[12] Rezeq M, Eledlebi K, Lababidi I, Ismail M. Analysis of the interface barriers between nano metal particles and semiconductors substrates. In *2013 IEEE 56th International Midwest Symposium on Circuits and Systems (MWSCAS)*, OH, USA, 2013.
[13] Rezeq M, Eledlebi K, Ismail M. Characterization of nano Schottky junctions for a new structure of nano-electronic devices. In *IEEE Nano 2014*, Toronto, Canada, 2014.
[14] Rezeq M, Eledlebi K, Ismail M. Characterization of nano scale metal Schottky contacts with silicon substrates for scaling of electronic devices. In *Micro and Nano Engineering (MNE 2014)*, Lausanne, Switzerland, 2014.
[15] Eledlebi K, Rezeq M, Ismail M. Numerical analysis of nano Schottky junctions for developing novel sub-20 nm electronic devices. In *21st IEEE International Conference on Electronics Circuits and Systems (ICECS 2014)*, Marseilles, France, 2014.
[16] Pierret RF. MS contacts and Schottky diodes, field effect transistors – the J-Fet and MESFET. In *Semiconductor Device Fundamentals*. Addison-Wesley: CA, 1996, pp. 477–483, 530–550.
[17] Zeghbroeck BV. *Principles of Semiconductor Devices*. ECEE: Colorado, December 2011. [Online]. Available: http://ecee.colorado.edu/~bart/book/book/chapter4/ch4_2.htm#fig4_2_4. Accessed 27 September, 2013.
[18] Aubry V, Meyer F. Schottky diodes with high series resistance: limitations of forward I-V methods. *Appl. Phys.* 1994, 78, 7973–7984.
[19] Dhiraj S, Ji Ung L. Ideal graphene/silicon Schottky junction diodes. *Nano Lett.* 2014, 14, 4660–4664.
[20] Wu C, Zhang Z, Wu Y, Lv P, Nie B, Luo L, Wang L, Hu J, Jie J, Flexible CuS nanotubes-ITO film Schottky junction solar cells with enhanced light harvesting by using an Ag mirror. *Nanotechnology* 2013, 24, 045402.
[21] Sze SM. *Physics of Semiconductor Devices*. Wiley-Interscience Publication: NJ, 1981.
[22] Hiesgen R, Krause M, Meissner D. STM measurement of current-potential curves at a semiconductor surface. *Electrochim. Acta* 2000, 45, 3213–3223.
[23] Kulkka MA, Li W, Kavanagh KL, Yu H-Z. Nanoscale electrical and structural characterization of gold/alkyl monolayer/silicon diode junctions. *J. Phys. Chem.* 2008, 112, 9081–9088.
[24] Nörenberg C, Myhra S, Dobson P. Scanning probe microscopy studies on the growth of palladium and nickel on GaN(0001). *J. Phys. Conf. Ser. (IOP Sci.)* 2010, 209, 1–4.
[25] Song JQ, Ding T, Li J, Cai Q. Scanning tunneling microscope study of nanosized metal-semiconductor contacts between $ErSi_2$ nanoislands and Si(0 0 1) substrate. *Surf. Sci.* 2010, 604, 361–365.